A Terrain-Following Coordinate with Smoothed Coordinate Surfaces

J. B. KLEMP

National Center for Atmospheric Research, Boulder, Colorado*

(Manuscript received 18 November 2010, in final form 15 February 2011)

ABSTRACT

An alternative form for a height-based terrain-following coordinate is presented here that progressively smoothes the coordinate surfaces with height to remove smaller scale (steeper) terrain structure from the surfaces. Testing this approach in comparison with traditional and hybrid terrain-following formulations in resting-atmosphere simulations demonstrates that it can significantly reduce artificial circulations caused by inaccuracies in the horizontal pressure gradient term. The simulations also suggest that some further improvement in the accuracy of the horizontal pressure gradient terms can be achieved using a simplified version of Mahrer's approach, which can be implemented with little increase in computational cost or complexity.

1. Introduction

The treatment of terrain in atmospheric numerical models is commonly handled through the use of a terrain-following vertical coordinate. Although this form of vertical coordinate has proven effective in a wide variety of applications, it is recognized that the accuracy in representing the horizontal pressure gradient is diminished above regions of relatively steep terrain, which can potentially produce spurious small-scale circulations (an issue even in large-scale hydrostatic models). To help mitigate these effects, various modifications to the basic terrain-following coordinate formulation have been introduced that more rapidly remove terrain influences in the coordinate surfaces with increasing height. This study describes another alternative for modifying the terrain-following coordinate that may provide some additional benefit in reducing artificial terrain-induced behavior.

The basic terrain-following (BTF) coordinate as introduced by Gal-Chen and Somerville (1975) has the form

$$z = (z_t - h)\frac{\zeta}{z_t} + h = \zeta + \left(1 - \frac{\zeta}{z_t}\right)h, \qquad (1)$$

where $z(x, y, \zeta)$ represents the height of coordinate surfaces defined by constant values of ζ and $h(x, y)$ is the terrain height. With this coordinate transformation the influence of the terrain decreases linearly with height, from terrain-following at the surface ($\zeta = 0$) to a rigid lid at the top of the model domain ($\zeta = z_t$).

Arakawa and Lamb (1977) and Simmons and Burridge (1981) recognized that the vertical coordinate could be specified such that it is terrain following at the surface, but with more flexible control over the reduction of terrain influence on the coordinate surfaces with increasing height. This hybrid terrain-following (HTF) coordinate can be expressed in a form complementary to (1) as

$$z = (z_t - A'h)\frac{\zeta}{z_t} + A'h = \zeta + Ah, \qquad (2)$$

where $A(\zeta)$ [or $A' = A/(1 - \zeta/z_t)$] controls the rate at which the coordinate transitions from terrain following at the surface toward constant height surfaces aloft. For $A(\zeta) = 1 - \zeta/z_t$ (i.e., $A' = 1$) the coordinate reverts to the BTF formulation (1), while for $A(\zeta) = 0$ the coordinates coincide with constant height surfaces. Thus, the profile for $A(\zeta)$ can be specified to transition the vertical coordinate from terrain following at the surface toward constant height surfaces aloft more rapidly than in the BTF formulation (1).

More recently, Schär et al. (2002) (and revisited by Leuenberger et al. 2010) proposed a modified terrain-following hybrid coordinate that allows smaller-scale terrain influences on the coordinate surfaces to be removed

* The National Center for Atmospheric Research is sponsored by the National Science Foundation.

Corresponding author address: Dr. Joseph B. Klemp, National Center for Atmospheric Research, Boulder, CO 80307-3000.
E-mail: klemp@ucar.edu

DOI: 10.1175/MWR-D-10-05046.1

more rapidly with height than can be accommodated in the pure hybrid coordinate (2). In this approach, named the Smooth Level Vertical (SLEVE) coordinate, the actual terrain $h(x, y)$ is divided into two components: an appropriately smoothed representation of the terrain $h_1(x, y)$ and the remainder $h_2(x, y) = h - h_1$, which contains most of the smaller-scale terrain structure. Writing the SLEVE coordinate in the form

$$z = \zeta + h_1 b_1(\zeta) + h_2 b_2(\zeta) \tag{3}$$

allows the smaller-scale terrain influences to be removed more rapidly with height than the larger-scale influences. Each portion of the terrain is treated in the same manner as a hybrid coordinate, but with a profile for $b_2(\zeta)$ that decreases much faster with height than $b_1(\zeta)$, subject to the constraint that $b_1(0) = b_2(0) = 1$. The rate at which terrain influences can be removed from a terrain-following coordinate is constrained by the need to keep the vertical spacing between adjacent coordinate surfaces from becoming too small (or negative). Since the maximum height of h_2 will be less than the maximum height of the full terrain h, a more rapid decay in the influence of h_2 on the coordinate surfaces can be achieved than would be possible if a single decay rate were applied to the full terrain profile.

In this study, a further modification to the construction of a terrain-following coordinate is proposed that allows more flexible control over terrain influences by directly smoothing the coordinate surfaces to progressively remove smaller-scale terrain structure from these surfaces with increasing height above the ground. This coordinate-surface smoothing can then be combined with a hybrid approach to provide further flexibility in constructing a terrain-following vertical coordinate to enhance numerical accuracy. The description of the approach will be presented in section 2 with a demonstration in section 3 of its performance in comparison with other coordinate formulations for a resting-atmosphere simulation. Section 4 will briefly discuss the sensitivity of the calculation of the horizontal pressure gradients to an alternative numerical representation.

2. Formulation for smoothed terrain-following coordinate surfaces

In the alternative terrain-following coordinate proposed here, the objective is to reduce smaller-scale terrain influences by progressively smoothing coordinate surfaces with increasing height above the terrain. This is accomplished through a simple modification of the BTF formulation (2) to the more general expression:

$$z = (z_t - A' h_s)\frac{\zeta}{z_t} + A' h_s = \zeta + A h_s. \tag{4}$$

Here, $h_s(x, y, \zeta)$ represents the terrain influence in the vertical-coordinate definition, with $h_s(x, y, 0) = h(x, y)$, and for $h_s \equiv h$, (4) reverts to the HTF coordinate (2). However, (4) has the added flexibility that h_s can be specified to be a smoother representation of h, with an increasing amount of smoothing applied at increasing levels of ζ. Although (4) could be further simplified by folding $A(\zeta)$ into h_s, it seems beneficial to specify separately the attenuation of overall terrain influence with height A from the amount of terrain smoothing h_s in the vertical coordinate.

A variety of techniques can be considered in constructing the smoothed h_s surfaces, including Fourier filtering to selectively remove higher wavenumber influences with increasing height, or a multipass local smoother of the form

$$h_s^{(n)} = h_s^{(n-1)} + \beta(\zeta) d^2 \nabla_\zeta^2 h_s^{(n-1)}, \tag{5}$$

where ∇_ζ^2 is the Laplacian evaluated at constant ζ, $\beta(\zeta)$ is the dimensionless smoothing coefficient, and d is a characteristic gridcell dimension. To illustrate the application of this approach, the use of (5) will be described for a two-dimensional (x, z) model domain. Starting from the surface where $h_s(x, 0) = h(x)$, iterations at each successively higher level of ζ_k begin with $h_{s\,i,k}^{(0)} = h_{s\,i,k-1}$, and proceed by applying the smoothing operator

$$h_{s\,i,k}^{(n)} = h_{s\,i,k}^{(n-1)} + \beta_k\left[h_{s\,i+1,k}^{(n-1)} - 2h_{s\,i,k}^{(n-1)} + h_{s\,i-1,k}^{(n-1)}\right], \tag{6}$$

where the subscripts i and k denote the horizontal and vertical grid indices, respectively, such that $h_{s\,i,k} = h_s(x_i, \zeta_k)$. At each level, a specified number of iterations M_k ($M_k = 50$ for the applications tested here) are applied as long as the minimum vertical grid spacing does not drop below a prescribed minimum. Based on (4), this limit requires

$$\zeta_k + A_k h_{s\,i,k}^{(n)} - (\zeta_{k-1} + A_{k-1} h_{s\,i,k-1}) \geq \gamma_{\min}(\zeta_k - \zeta_{k-1}) \tag{7}$$

for all i, where $\gamma_{\min}$ is the specified minimum allowed fractional grid spacing, $\Delta z_k/\Delta\zeta_k$. When the terrain contains significant small-scale structure, a small amount of smoothing can produce relatively large changes in $h_s^{(n)}$, particularly near the ground. Therefore, in the current testing β_k is scaled by the nominal coordinate surface

height ζ_k relative to the maximum terrain height h_m using the expression

$$\beta_k = 0.2 \min\left(\frac{\zeta_k}{2h_m}, 1\right). \tag{8}$$

These smoothing parameters (M_k, β_k, and $\gamma_{\min}$) may require modification depending on the particular application, as discussed further in the summary.

In specifying the hybrid attenuation profile $A(\zeta)$, the objective is to decrease the terrain influence (decrease A) as rapidly as possible with height without producing vertical grid spacings that get too small. After some experimentation, the profile

$$\begin{aligned} A(\zeta) &= \cos^6\left(\frac{\pi}{2}\frac{\zeta}{z_H}\right) \quad \text{for} \quad \zeta < z_H \\ A(\zeta) &= 0 \qquad\qquad\qquad\quad \text{for} \quad \zeta \geq z_H \end{aligned} \tag{9}$$

appears to provide a reasonable balance between these desired characteristics, with the rate of attenuation regulated by the parameter z_H. For a pure hybrid coordinate z_H can be specified to achieve a desired $\gamma_{\min}$ by differentiating (4) with $h_s = h$ and using (9):

$$\frac{\partial z}{\partial \zeta} = 1 - 3\pi\frac{h_m}{z_H}\cos^5\left(\frac{\pi}{2}\frac{\zeta}{z_H}\right)\sin\left(\frac{\pi}{2}\frac{\zeta}{z_H}\right) \geq \gamma_{\min}. \tag{10}$$

At the point where $\partial z/\partial\zeta$ is a minimum [$\zeta/z_H = (2/\pi)\sin^{-1}(1/\sqrt{6})$], (10) yields

$$\frac{z_H}{h_m} = \frac{2.44}{1 - \gamma_{\min}}. \tag{11}$$

When including terrain smoothing in (4), this constraint must be further relaxed (z_H/h_m further increased) to allow sufficient smoothing while satisfying the constraint (7).

3. Simulation for a resting atmosphere

To illustrate a practical application of this smoothed terrain-following (STF) coordinate, results will be presented for resting-atmosphere simulations designed to challenge the accuracy of the horizontal pressure-gradient computations. Initializing the model with a horizontally homogeneous thermodynamic sounding, an atmosphere initially at rest should remain motionless throughout the numerical integration. The simulations are conducted for a 2D atmosphere using model numerics as described by Klemp et al. (2007) for a height-based terrain-following coordinate. To accommodate the HTF or STF coordinate, the only modification to these numerics is to allow the metric $\partial\zeta/\partial z$ to be a function of both x and ζ instead of depending only on x.

The terrain profile specified for these simulations follows the form used by Schär et al. (2002) for their mountain-wave simulations:

$$h(x) = h_m \exp\left[-\left(\frac{x}{a}\right)^2\right]\cos^2\left(\frac{\pi x}{\lambda}\right), \tag{12}$$

where $a = 5$ km, $\lambda = 4$ km, and here we set $h_m = 1000$ m.

In the model numerics, the horizontal pressure-gradient term in the flux-form representation of the horizontal momentum equation with C-grid staggering is given by

$$z_\zeta \left.\frac{\partial p}{\partial x}\right|_z = \delta_x(p z_\zeta) - \delta_\zeta(\overline{\overline{p}^{x}}^{\zeta} z_x), \tag{13}$$

where $z_x = \delta_x z$ and $z_\zeta = \delta_\zeta z$ are the metrics of the transformed vertical coordinate. Here, δ_x is the finite-difference operator over one grid interval in the x direction at constant ζ, and similarly for δ_ζ. In computing the horizontal pressure gradient according to (13), the pressure gradient along a constant ζ surface (first term on the rhs) is adjusted back to constant height using the vertical pressure gradient and the coordinate-surface slope (second term on rhs). Thus, the errors in approximating the horizontal pressure gradients will be minimized when the vertical pressure gradients are nearly linear. To include a more complex structure in the lower-level vertical pressure gradients for the resting-atmosphere simulations, the specified thermodynamic sounding has constant stability ($N = 0.01$ s^{-1}) throughout, but with the addition of an inversion layer ($N = 0.02$ s^{-1} for $2 \leq z \leq 3$ km). In the model equations, the thermodynamic variables are expressed as perturbations from a reference sounding to reduce numerical error in the pressure-gradient terms (Klemp et al. 2007). Here, it is important to define a reference sounding that differs from the actual sounding to allow nonzero perturbations. Hence, the specified reference sounding corresponds to an adiabatic atmosphere ($\theta_0 = 288$ K).

Simulations for the prescribed terrain (12) and atmospheric sounding were conducted for several different horizontal and vertical resolutions. These tests indicate that for a given vertical grid structure, the magnitude of evolving artificial circulations is not strongly dependent on the horizontal resolution over the range $\Delta x = 250$–1000 m. However, these artificial circulations are found to be highly dependent on the vertical resolution, with amplitudes that decrease dramatically with decreasing $\Delta\zeta$ until $\Delta\zeta$ reaches about 100 m. This overall behavior suggests that the accuracy of the $\partial p/\partial\zeta$ term in (13) dominates the accuracy of the horizontal pressure gradient calculation for the terrain slopes and grid regimes tested here

(cf. error analysis by Dempsey and Davis 1998). As pointed out by Mahrer (1984), errors in the horizontal pressure gradient may increase particularly when the coordinate slope z_x becomes significantly greater than the ratio of the grid increments $\Delta z/\Delta x$. However, for this resting-atmosphere case, artificial circulations remain small (maximum vertical velocities less than 0.1 m s^{-1} for the BTF case for vertical grids as small as $\Delta\zeta = 25$ m). For the simulations presented here, the grid increments are $\Delta x = 500$ m and $\Delta\zeta = 500$ m, with the vertical grid resolution intentionally chosen to be rather coarse to challenge the numerical accuracy. The computational domain dimensions are 200 km in the horizontal with open lateral boundary conditions and $z_t = 20$ km. A small constant eddy diffusion ($K_m = 10$ m^2 s^{-1}) is also included to remove small-scale noise that would inevitably be filtered in any practical model applications.

Using the BTF coordinate (1) and the model configuration described above, only about one-quarter of the terrain influence has been removed at $z = 5$ km, the top of the displayed portion of the domain in Fig. 1a. Over the 5-h simulation, strong circulations develop that produce significant distortions in the potential temperature field (Fig. 1b) with maximum vertical velocities that reach ~10 m s^{-1} (Fig. 2). Enabling the HTF coordinate (2) with $A(\zeta)$ defined by (9) with $z_H = 5$ km, the terrain influence in the vertical coordinate has been completely removed over the lowest 5 km as shown in Fig. 1c. Distortions in the potential temperature field (Fig. 1d) are reduced significantly from those in the BTF simulation, although the maximum vertical velocity perturbation still reach several meters per second (Fig. 2). In Fig. 1e, the coordinate surfaces are displayed for the STF simulation, produced using (4) and (9) with $z_H = 8$ km, and constructing $h_s(x, \zeta)$ by iteratively applying (6) and (7) for $\gamma_{\min} = 0.6$ as described in the previous section. Here again the terrain influence is essentially removed in the lowest 5 km, but in addition, the influence of the smaller-scale terrain structure is nearly absent above $z = 2$ km. For this simulation, there is little disturbance of the potential temperature field (Fig. 1f) and the maximum vertical velocities do not exceed several tenths of a meter per second (Fig. 2). Simulating this case with coordinate smoothing as described above but with no hybrid attenuation ($A = 1 - \zeta/z_t$), produced perturbations (not shown) only slightly larger than those just discussed that also included hybrid attenuation with $z_H = 8$ km (Figs. 1f and 2 for STF).

For comparison, this case was also simulated using the SLEVE coordinate (3). Following Schär et al. (2002), the terrain profile $h(x)$ in (12) is partitioned into a larger-scale segment:

$$h_1(x) = \frac{1}{2} h_m \exp\left[-\left(\frac{x}{a}\right)^2\right], \tag{14}$$

and a second portion $h_2 = h - h_1$ containing the smaller-scale structure. The decay functions $b_1(\zeta)$ and $b_2(\zeta)$ are specified following Leuenberger et al. (2010), using their Eq. (2) with $s_1 = 4$ km, $s_2 = 1$ km, and the exponent $n = 1.35$, corresponding to their optimal value. These parameters yield $\gamma_{\min} = 0.6$, the same as in the STF case. This coordinate formulation also produces significantly smaller perturbations (Figs. 1h and 2) than those in the HTF simulation, though not quite as small as those obtained with the STF coordinate.

4. Numerical treatment of the horizontal pressure gradient

In computing the horizontal pressure gradients, the formulation (13) adjusts the pressure gradient to constant height using a centered difference for the vertical pressure gradient [second term on rhs of (13)]. As proposed by Mahrer (1984) and analyzed by Dempsey and Davis (1998), the accuracy of this pressure gradient term can be improved (particularly for steep terrain) by expressing the pressure gradient (illustrated for 2D) in the form

$$\left.\frac{\partial p}{\partial x}\right|_z = \frac{1}{\Delta x}(p^*_{i+1/2,k} - p^*_{i-1/2,k}), \tag{15}$$

where $p^*_{i\pm1/2,k}$ represents pressure at the same height z as the horizontal velocity $u_{i,k}$, and is interpolated vertically between the two grid levels that bracket this height at $i \pm 1/2$ as illustrated in Fig. 3. Here, a simpler version of this technique is tested, in which $p^*_{i\pm1/2,k}$ is linearly interpolated (or extrapolated) using $p_{i\pm1/2,k}$ and the adjacent pressure above or below this level, depending on the slope of the coordinate surface:

$$\begin{aligned} p^*_{i+1/2,k} &= p_{i+1/2,k} \\ &\quad - \Delta z^*_{i,k}\left(\frac{p_{i+1/2,k-s+1/2} - p_{i+1/2,k-s-1/2}}{z_{i+1/2,k-s+1/2} - z_{i+1/2,k-s-1/2}}\right) \\ p^*_{i-1/2,k} &= p_{i-1/2,k} \\ &\quad + \Delta z^*_{i,k}\left(\frac{p_{i-1/2,k+s+1/2} - p_{i-1/2,k+s-1/2}}{z_{i-1/2,k+s+1/2} - z_{i-1/2,k+s-1/2}}\right), \end{aligned} \tag{16}$$

where $\Delta z^*_{i,k} = 1/2(z_{i+1/2,k} - z_{i-1/2,k})$ and index $s = 1/2$ sign$(\Delta z^*_{i,k})$. At the lowest grid level, $p^*_{i\pm1/2,1}$ is obtained from a vertical quadratic interpolation using the lowest three grid levels.

This representation is the same as Mahrer's (1984) approach for up to moderate coordinate slopes (as shown in Fig. 3), but is less accurate for steep slopes where the target

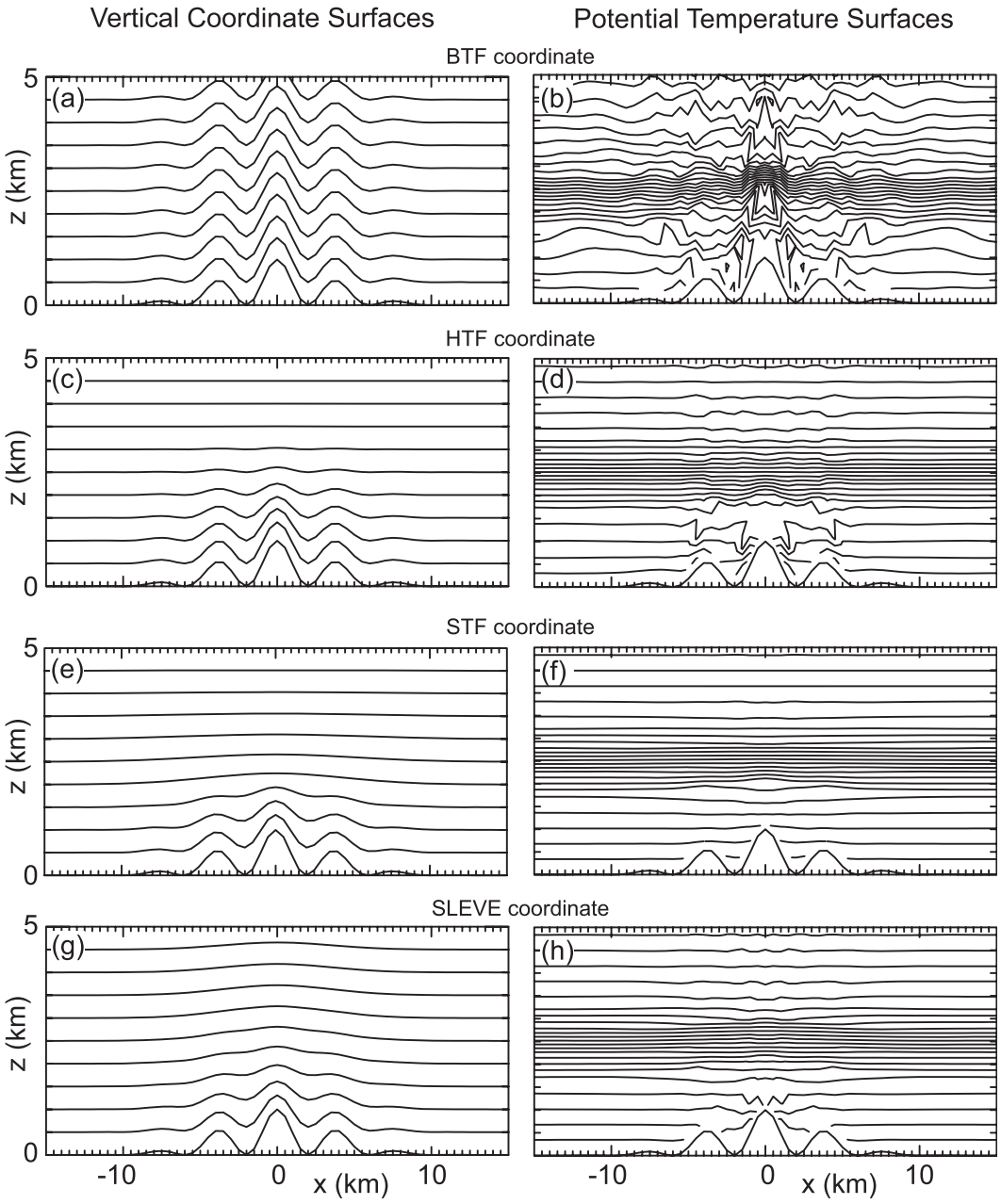

FIG. 1. Coordinate surfaces and potential temperature contours (contour interval 1 K) for the resting-atmosphere case described in section 3 for (a),(b) the BTF coordinate; (c),(d) the HTF coordinate; (e),(f) the STF coordinate; and (g),(h) the SLEVE coordinate. Note that the top of the model domain is at $z = 20$ km.

constant height interpolation level is more than one grid interval above or below level k at $i \pm 1/2$. However, it does not require the computation and storage of the indices that bracket the constant height levels on either side of all of the horizontal velocity grid points. The scheme is easy to implement, has little additional computational cost, and, by interpolating $p^*_{i\pm1/2,k}$ over one vertical grid interval, should be more accurate than (13) in adjusting the pressure-gradient term to constant height. [The numerical representation in (13) can be rearranged to a similar form as (15) and (16), except with the vertical pressure gradient taken over two grid intervals instead of one as in (16).] As shown in Fig. 4, the increased accuracy is confirmed in the resting-atmosphere simulation described in the previous section as the maximum vertical velocities are significantly reduced for all of the terrain-following coordinate representations from those produced using (13) to compute the horizontal pressure gradient (Fig. 2). Simulations (not

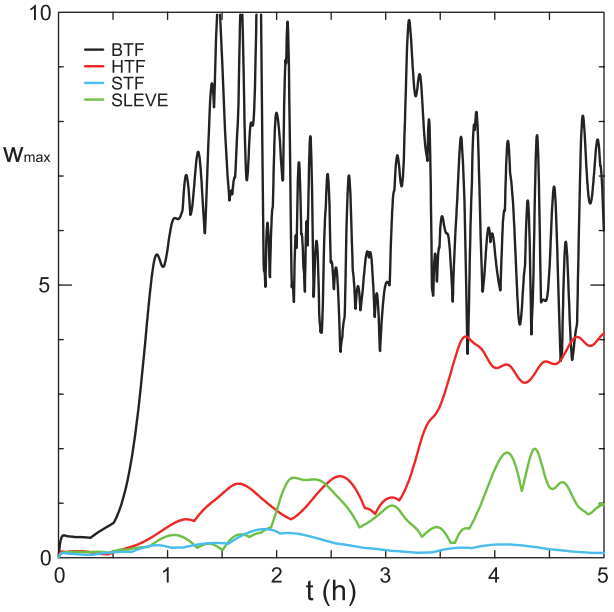

FIG. 2. Time series of the maximum vertical velocity for the resting-atmosphere simulations in Fig. 1 for the BTF coordinate (black), the HTF coordinate (red), the STF coordinate (turquoise), and the SLEVE coordinate (green).

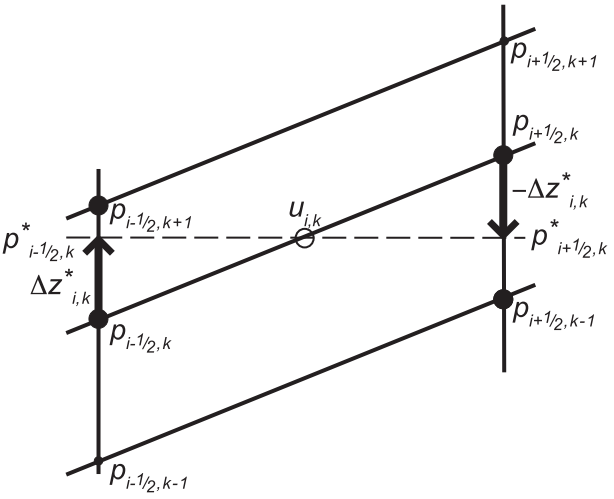

FIG. 3. Schematic illustrating the interpolation of pressure to constant height in computing the horizontal pressure gradient with sloping coordinate surfaces.

shown) with a vertically stretched grid (about an order of magnitude increase in the grid size from the surface to the model top) exhibited similar relative reductions in the resting-atmosphere perturbations using the pressure-gradient formulation (15)–(16). Further testing with this simplified Mahrer approach suggests that for steeper terrain, it allows somewhat larger time steps for the acoustic terms in a split-explicit time integration scheme than the restricted stability limit using (13) to evaluate the horizontal pressure gradients (see Steppeler 1995 and Dudhia 1995).

5. Summary

The terrain-following coordinate proposed here is intended to provide additional flexibility in reducing the influence of the terrain (particularly steep terrain) on the coordinate surfaces. With this approach the form of the coordinate transform is similar to those of basic and hybrid terrain-following coordinates, but includes smoothing of the coordinate surfaces that progressively removes smaller-scale structure with increasing height above the terrain. This direct smoothing of coordinate surfaces represents a significant difference from the SLEVE coordinate proposed by Schär et al. (2002), in which the terrain h is separated into a large-scale profile h_1 and a residual that contains much of the smaller-scale structure h_2. Following this decomposition, the SLEVE approach attenuates the influence of all scales in the h_1 profile at the same rate with increasing height (through the hybrid parameter s_1) while all scales in the h_2 portion are attenuated at the same rate (regulated by s_2). For $s_2 < s_1$, the h_2 contribution to the coordinate surfaces is removed more rapidly with height than the h_1 portion, but within each of the two profiles there is no selective scale removal. Thus, the STF coordinate appears to provide more flexibility in providing scale-selective attenuation of terrain influences on the coordinate surfaces across

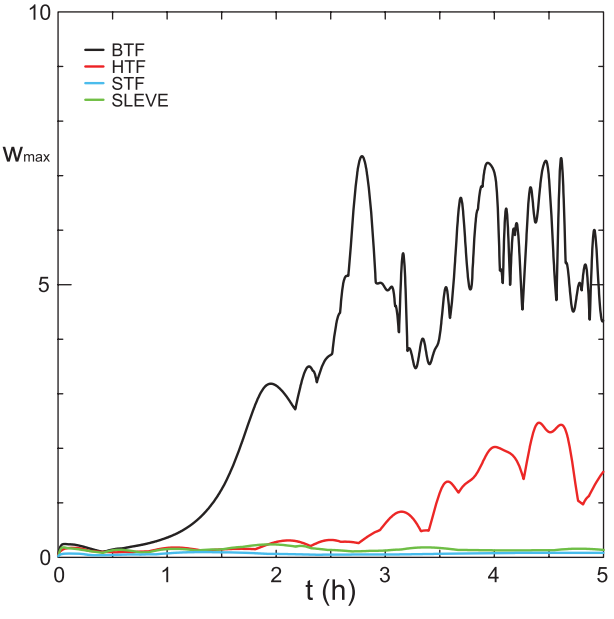

FIG. 4. As in Fig. 2, but using a simplified version of Mahrer's technique for computing the horizontal pressure gradient, as expressed in (16).

the full range of terrain scales. (In principle, the influence of each wavenumber contribution to the terrain could be independently filtered with height.)

In the resting-atmosphere simulations described in the previous section, the STF coordinate demonstrates a significant reduction in the artificial circulations from those arising with the basic or hybrid terrain-following coordinates and some further improvement over the SLEVE coordinate. These simulations were intentionally conducted with fairly coarse vertical grid resolution. For simulations with higher vertical resolution near the surface, using either a constant or stretched grid, the amplitudes of perturbations drop rapidly as the resolution increases. However, simulations with the BTF, HTF, STF, and SLEVE coordinates exhibit the same relative behavior as the simulations in section 3. Additional resting-atmosphere and mountain-wave simulations (including variable vertical resolution) have been conducted that further confirm the efficacy of this smoothed-coordinate technique.

As for the SLEVE coordinate, the STF coordinate requires specification of a number of parameters to regulate the rate of smoothing and terrain decay with height (set by the parameters M_k, β_k, $\gamma_{\min}$, and z_H). Some amount of experimentation will inevitably be needed in choosing the "best" combination of parameters for a particular application. Some guidance based on admittedly limited experience may be helpful to those who might consider trying this coordinate technique. The parameter $M_k(\zeta)$ specifies the maximum number of smoothing iterations for each coordinate surface. This should be reasonably large to allow smoothing effects to be distributed over wide distances, but results seem to be only weakly dependent on M_k for values above about 20. The profile $\beta_k(\zeta)$ defines the second-order smoothing coefficient in (5); it should be small enough to allow a reasonable number of smoothing iterations ($\sim$10) at lower coordinate levels before reaching the specified $\gamma_{\min}$. The profile for β_k defined in (8) seems to work well in a variety of 2D applications; in preliminary testing in 3D for real terrain, better results were obtained using values about one-half those defined in (8). For the minimum coordinate spacing $\gamma_{\min}$, values of 0.5–0.6 seem to work best in 2D applications, while values about half this magnitude appear better for 3D real-terrain simulations. Finally, for the depth of the hybrid terrain attenuation z_H, as long as it is at least about 25% larger than the minimum value for the pure hybrid coordinate as defined in (11), results do not appear to be strongly dependent on the value chosen. In fact, as mentioned in the previous section, utilizing only the smoothing portion of the coordinate specification ($A = 1 - \zeta/z_t$) does not seem to significantly compromise the results.

This STF coordinate is particularly well suited for a height-based vertical coordinate in which the coordinate surfaces remain fixed over time, since smoothed $h_s(x, y, \zeta)$ surfaces need only be computed once, during model initialization. For a pressure-based coordinate, smoothed coordinate surfaces would need to be continually recomputed because of the variation of the surface pressure with time.

Evaluating the horizontal pressure gradients using a simplified version (16) of Mahrer's (1984) scheme appears to improve the numerical accuracy over the representation (13) with little impact on code efficiency or complexity. This improvement arises primarily from the decrease in the vertical interval over which pressure is interpolated to provide a pressure gradient at constant height, and is realized even for terrain that is not steeply sloped.

Acknowledgments. The author would like to thank Bill Skamarock for his helpful suggestions and Günther Zängl and an anonymous reviewer for their careful reviews of this paper.

REFERENCES

Arakawa, A., and V. R. Lamb, 1977: Computational design of the basic dynamical processes of the UCLA general circulation model. *Methods in Computational Physics,* Vol. 17, J. Chang, Ed., Academic Press, 173–265.

Dempsey, D., and C. Davis, 1998: Error analysis and tests of pressure-gradient force schemes in a nonhydrostatic, mesoscale model. Preprints, *12th Conf. on Numerical Weather Prediction,* Phoenix, AZ, Amer. Meteor. Soc., 236–239.

Dudhia, J., 1995: Reply. *Mon. Wea. Rev.,* **123,** 2573–2575.

Gal-Chen, T., and R. Somerville, 1975: On the use of a coordinate transformation for the solution of the Navier-Stokes equations. *J. Comput. Phys.,* **17,** 209–228.

Klemp, J. B., W. C. Skamarock, and J. Dudhia, 2007: Conservative split-explicit time integration methods for the compressible nonhydrostatic equations. *Mon. Wea. Rev.,* **135,** 2897–2913.

Leuenberger, D., M. Koller, O. Fuhrer, and C. Schär, 2010: A generalization of the SLEVE vertical coordinate. *Mon. Wea. Rev.,* **138,** 3683–3689.

Mahrer, Y., 1984: An improved numerical approximation of the horizontal gradients in a terrain-following coordinate system. *Mon. Wea. Rev.,* **112,** 918–922.

Schär, C., D. Leuenberger, O. Fuhrer, D. Lüthi, and C. Girard, 2002: A new terrain-following vertical coordinate formulation for atmospheric prediction models. *Mon. Wea. Rev.,* **130,** 2459–2480.

Simmons, A. J., and D. M. Burridge, 1981: An energy and angular-momentum conserving finite-difference scheme and hybrid vertical coordinates. *Mon. Wea. Rev.,* **109,** 758–766.

Steppeler, J., 1995: Comments on "A nonhydrostatic version of the Penn State–NCAR Mesoscale Model: Validation tests and simulation of an Atlantic cyclone and cold front." *Mon. Wea. Rev.,* **123,** 2572.